

Charge disproportionation and search for orbital ordering in NdNiO_3 by use of resonant x-ray diffraction

V. Scagnoli,* U. Staub, M. Janousch, A. M. Mulders, and M. Shi
Swiss Light Source, Paul Scherrer Institut, CH-5232, Villigen PSI, Switzerland

G. I. Meijer
IBM Research, Zurich Research Laboratory, CH-8803 Rüschlikon, Switzerland

S. Rosenkranz
Materials Science Division, Argonne National Laboratory, Argonne, Illinois 60439, USA

S. B. Wilkins
European Commission, Joint Research Center, Institute for Transuranium Elements, Hermann von Helmholtz-Platz 1, 76344 Eggenstein-Leopoldshafen, Germany
and European Synchrotron Radiation Facility, BP 220, F-38043 Grenoble Cedex, France

L. Paolasini
European Synchrotron Radiation Facility, BP 220, F-38043 Grenoble Cedex, France

J. Karpinski and S. M. Kazakov
Laboratorium für Festkörperphysik, ETH-Zürich, CH-8093 Zürich, Switzerland

S. W. Lovesey
Diamond Light Source Ltd. and ISIS Facility, Rutherford Appleton Laboratory, Chilton, Oxfordshire OX11 0QX, United Kingdom
 (Received 26 April 2005; revised manuscript received 11 July 2005; published 14 October 2005)

Detailed resonant x-ray diffraction experiments including azimuthal angle scans were performed on NdNiO_3 around the Ni K absorption edge, allowing us to investigate the electronic changes associated with the metal-to-insulator transition. The influence on the observed reflections of charge disproportionation and the asphericity of the Ni electron density is evaluated. The asphericity, due to the distortion of the oxygen octahedra, persists also in the metallic phase, but its influence on the unrotated σ - σ (033) diffraction signal is found to be negligible, in contrast to the case for the superlattice reflections found in manganites and magnetite. We conclude that the σ - σ scattering intensity is consistent with charge disproportionation at the Ni site. No (1/2 0 1/2) type reflections were found, making unlikely the simultaneous occurrence of orbital order with this previously proposed wave vector. Moreover, the asphericity observed in the $4p$ shell in the metallic state indicates that there is no orbital degeneracy. Therefore, no orbital ordering is expected to occur at the metal-insulator transition.

DOI: [10.1103/PhysRevB.72.155111](https://doi.org/10.1103/PhysRevB.72.155111)

PACS number(s): 78.70.Ck, 71.30.+h

I. INTRODUCTION

The $3d$ transition-metal oxides exhibit a fascinating variety of physical properties, ranging from high- T_c superconductivity to colossal magnetoresistance. These strongly correlated electron systems often show metal-to-insulator transitions, whose microscopic origin is of on-going interest. Many are Mott insulators with a half-filled $3d$ band, for which the electron cannot hop to neighboring atoms. Spin and orbital degrees of freedom may survive and can play a significant role in the metal-insulator transitions. Particular interesting cases are those temperature driven metal-insulator transitions at which the itinerant charge carriers become localized. This occurs in various transition-metal oxides such as manganites,¹ cobaltides,²⁻⁴ or nickelates,^{5,6} but also in other oxides such as magnetite.^{7,8} The interplay and the competition between charge, orbital, and spin degrees of freedom

can lead to charge and orbital ordered ground states for which the electrons are localized.

Recent resonant x-ray scattering (RXS) experiments have challenged the interpretation of charge ordering (CO) of the Fe^{2+} and Fe^{3+} ions in magnetite below the Verwey transition.^{9,10} The azimuthal and energy dependence of certain superlattice reflections have been explained with a model without ionic charge order, which contradicts the CO model of Verwey.^{7,8} Doubts about charge ordering have also been raised for manganites.¹¹⁻¹³ The observation of forbidden reflections by means of RXS was first interpreted as “direct” evidence for CO and orbital ordering (OO),^{14,15} and a model was proposed based on CO at two different Mn sites, i.e., $\text{Mn}_{\text{I}}=3+$ and $\text{Mn}_{\text{II}}=4+$, and OO at the Mn_{I} site.¹⁶ Subsequent studies showed that the anisotropy of the scattering tensor must be taken into account to describe the azimuthal angle dependence of the CO type reflections.^{12,13}

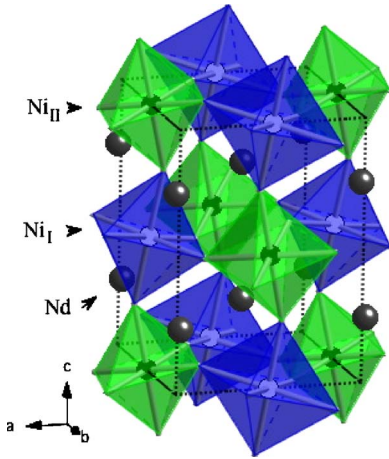


FIG. 1. (Color online) The proposed crystal structure below T_{MI} of $NdNiO_3$ with charge disproportionation. The two different Ni sites, Ni_I and Ni_{II} , with the corresponding oxygen octahedra (shaded) are drawn in different colors.

These studies challenged the simple CO picture for manganites and concluded that at most a fractional charge order exists (charge disproportionation). It is therefore interesting to investigate other transition metal oxides for which charge ordering has been claimed.

Charge order has been claimed first for $YNiO_3$ (Ref. 17) and then for $NdNiO_3$,¹⁸ two members of the $RNiO_3$ family, R being a trivalent rare-earth ion (La to Lu) or Y. At room temperature, $RNiO_3$ crystallizes in the orthorhombically distorted perovskite structure $Pbnm$, with unit cell $\sqrt{2}a_p \times \sqrt{2}a_p \times 2a_p$, where a_p is the perovskite cell parameter. The Ni ion has a nominal valence of 3+ and a $3d$ -electron configuration $t_{2g}^6 e_g^1$, with spin $S=1/2$. In its insulating state, $RNiO_3$ has a small charge-transfer energy and can be regarded as a self-doped Mott insulator.^{19,20} $RNiO_3$ exhibits a thermally driven metal-insulator transition at T_{MI} and a further transition to long-range antiferromagnetic order at $T_N \ll T_{MI}$.^{5,6} T_{MI} and T_N depend strongly on the size of the rare-earth ion. $T_{MI}=T_N$ for Nd and Pr. Associated with T_{MI} is a subtle expansion of the crystallographic unit cell, which causes a narrowing of the bandwidth, eventually leading to the opening of a gap at the Fermi surface.^{6,17,21} Particularly interesting is the magnetic behavior below T_N , where an unusual magnetic ordering with propagation vector $k=(1/2\ 0\ 1/2)$ has been found,²¹⁻²³ corresponding to an up-up-down-down stacking of the ferromagnetic planes along the pseudocubic $[111]$ direction. Because the twofold degenerate e_g orbital is singly occupied, a Jahn-Teller distortion and an orbital ordering ($d_{x^2-y^2}$ or $d_{3z^2-r^2}$) are expected in the insulating state.²⁴ However, no evidence for a Jahn-Teller distortion was found with neutron powder diffraction.²¹ Later it was suggested that the superstructure peaks due to the Jahn-Teller distortion might be too weak to be observed.²² $NdNiO_3$ could be an example among transition metal oxides, for which charge ordering occurs independently of orbital ordering. Recent resonant x-ray experiments indicated the presence of charge disproportionation in $NdNiO_3$.¹⁸ Figure 1 shows the crystal structure below T_{MI} ($P2_1/n$ space group), with the proposed charge disproportionation at the Ni sites

(Ni_I and Ni_{II}).²⁵ These results have been criticized,²⁶ as the resonance may be caused by the asphericity of the $4p$ shell similarly as for the manganites.²⁷ However, a careful study of the azimuthal angle dependence allows to distinguish between the two effects.

In order to address these critics, resonant x-ray scattering data on epitaxial films of $NdNiO_3$ with detailed azimuthal angle dependence are presented. They give clear evidence for charge disproportionation. A small asphericity of the Ni electronic states is already observed above T_{MI} which indicates that no orbital degeneracy exists in the e_g states. Therefore OO is unlikely to occur at T_{MI} .

II. EXPERIMENTAL DETAILS

High-quality epitaxial films of $NdNiO_3$ were grown on (001) and (011) oriented $NdGaO_3$ substrates ($Pbnm$) by pulsed laser deposition. Polycrystalline $NdNiO_3$, synthesized as in Ref. 5, was used as the ablation target. The films were deposited in 0.3 mbar oxygen atmosphere at $T=740$ °C. After deposition, the sample was cooled slowly in a controlled oxygen atmosphere of 1 bar. The energy of the KrF excimer laser was 800 mJ with 5 Hz repetition rate. The resistivity of the film was measured with the conventional 4-probe technique. The resistivity of the 500 Å thick $NdNiO_3$ (001) film shows a first-order metal-insulator transition at approximately $T=170$ and 150 K (see Fig. 1 of Ref. 18) upon heating and cooling, respectively. For a (011)-oriented thin film, the metal-to-insulator transition occurs at approximately $T=190$ and 170 K upon heating and cooling, respectively. T_{MI} is lower than in polycrystalline $NdNiO_3$, probably because of epitaxial strain. No impurity phases were detected with Cu $K\alpha$ x-ray diffraction. The rocking curve full width at half-maximum of the films was 0.14°. Synchrotron x-ray scattering experiments were performed at ID20 of the European Synchrotron Radiation Facility, Grenoble, France, in the vicinity of the Ni K -edge, at approximately 8.333 keV. The beamline energy resolution was 1 eV. A Cu (222) crystal was used for polarization analysis. For σ - π scattering, the suppression of the σ - σ channel was approximately 99.9%, and vice versa. The use of thin films has the advantage that their x-ray absorption is negligible, i.e., no absorption correction is required. The (033) and (105) reflections were studied using the [011] and [001] oriented films, respectively.

III. RESONANT X-RAY SCATTERING

RXS combines spectroscopy with diffraction and probes the presence of CO and OO in the hard^{12,14,15,18,28,29} and the soft³⁰⁻³² x-ray regions. For RXS, the incident photon energy is tuned to an absorption edge of an ion and probes its electronic state. At resonance the scattering is strongly enhanced and phenomena which are usually negligible, such as the asphericity of the atomic electron density and anisotropy of the tensor of scattering (ATS), can be observed. Investigation of the energy, polarization, and azimuthal angle (rotation about the scattering vector) dependence of Bragg peaks allows one to distinguish between these contributions. At resonance, the x-ray scattering factor is no longer a scalar, it must

be treated as an anisotropic tensor and depends on the point symmetry of the resonant ions.³³ For NdNiO₃, the scattering intensity at forbidden reflections can be ascribed to two different spherical x-ray scattering factors for the Ni ions, i.e., (1) charge disproportionation and/or (2) ATS arising from a distorted octahedral environment around the Ni ions (“dichroic effect”²⁶). The asphericity of the electron density can be significant in the case of chemical bonding (strong hybridization) and/or OO connected with Jahn-Teller distortions. The intensity arising from the spherical differences of the electronic state, can be caused by CO or by “spherically” different local coordinations.³⁴ When the asphericity is negligible, the spherical electron density approximation can be used. Within this approximation, the intensity of the diffracted beam is proportional to the square of the structure factor F ,

$$F(\mathbf{Q}, E) = \sum_{i=1}^n f_i(\mathbf{Q}, E) e^{i\mathbf{Q}\cdot\mathbf{R}_i} \delta(\mathbf{Q} - \tau), \quad (1)$$

neglecting the Debye-Waller term. Here \mathbf{Q} and E are the x-ray momentum transfer and the energy, respectively, $f_i(\mathbf{Q}, E)$ is the x-ray scattering factor of the i th ion at the position \mathbf{R}_i within the unit cell, and τ is a reciprocal lattice vector. The scattering factor can be written $f_i(\mathbf{Q}, E) = f_i^0(\mathbf{Q}) + f_i'(E) + if_i''(E)$, where $f_i^0(\mathbf{Q})$ is the Thompson scattering factor (atomic form factor) and $f_i'(E)$ and $f_i''(E)$ are the real and imaginary energy-dispersive correction factors, respectively. We define $\Delta f'_{\text{Ni}_I}(E) = f'_{\text{Ni}_I}(E) - f'_{\text{Ni}_{II}}(E)$ and $\Delta f''_{\text{Ni}_I}(E) = f''_{\text{Ni}_I}(E) - f''_{\text{Ni}_{II}}(E)$, with the ions Ni_I and Ni_{II} chosen as indicated in Fig. 1. For reflections of the type $(0kl)$ with k and l odd, the structure factor is

$$F_{0kl}(\mathbf{Q}, E) = A_{\text{O},\text{Nd}}(\mathbf{Q}) + 2\Delta f'_{\text{Ni}_I}(E) + 2i\Delta f''_{\text{Ni}_I}(E). \quad (2)$$

In the $Pbnm$ symmetry, oxygen and neodymium ions do not contribute to the scattering for these reflections. A similar structure factor can be obtained for $(h0l)$ type reflections with h and l odd.¹⁸ A nonzero, energy-dependent scattering intensity is expected for reflections $(0kl)$ and $(h0l)$ with both nonzero indices odd in case of charge disproportionation [$f'_{\text{Ni}_I}(E) \neq f'_{\text{Ni}_{II}}(E)$ and $f''_{\text{Ni}_I}(E) \neq f''_{\text{Ni}_{II}}(E)$]. In $Pbnm$ symmetry, without charge disproportionation, the structure factors are given by $F_{0kl} = 0$ and $F_{h0l} = A_{\text{O},\text{Nd}}(\mathbf{Q})$. If the spherical electron density approximation does not hold, the ATS contribution must be included. The structure factor F is then

$$F = \sum_{K, Q, q} (-1)^Q H_{-Q}^K D_{Qq}^K \Psi_q^K. \quad (3)$$

The first term H_{-Q}^K describes the dependence on the experimental geometry, D_{Qq}^K reflects a rotation of the local axes to those of the experimental geometry and Ψ_q^K is given by

$$\Psi_q^K = \sum_d e^{id\cdot\tau} \langle T_q^K \rangle_d, \quad (4)$$

where $\langle T_q^K \rangle_d$ is the spherical tensor which represents the electronic origin of the scattering. The positive integer K is the rank of the tensor, and the projection q can take the $(2K$

+1) integer values which satisfy $-K \leq q \leq K$. For a dipole transition, tensors up to rank 2 contribute ($K \leq 2$). $K=0$ reflects charge contribution, $K=1$ time-odd dipole, and $K=2$ time-even quadrupole, and can include a possible magnetic contribution in the paramagnetic phase. This description is applicable to the dipole transition at Ni K -edge ($1s \rightarrow 4p$) in NdNiO₃ with $Pbnm$ symmetry. For the $(0kl)$ and $(h0l)$ reflections with both nonzero indices odd, only $\langle T_q^2 \rangle_d$ terms with $q = \pm 1$ are nonzero, and $\langle T_1^2 \rangle_d = -\langle T_{-1}^2 \rangle_d^*$. This tensor contributes to both of the polarization channels σ - σ and σ - π and reflects the quadrupole $Q_{xz} + iQ_{yz}$ of the Ni $4p$ shell. For the $(h0l)$ reflection, there is an additional nonresonant contribution to the σ - σ channel arising from the oxygen and neodymium ions. This contribution, which has only a weak energy dependence in the vicinity of the Ni K -edge, can lead to interference with the resonant intensity.

The azimuthal angle ψ describes the sample rotation about the scattering wave vector. We define $\psi=0^\circ$ for the $[100]$ direction along the y axis of our experimental reference frame. The expressions for the structure factors for the $(0kl)$ and the $(h0l)$ reflections of NdNiO₃ are

$$F_{\sigma\text{-}\sigma}^{0kl}(\psi) = \langle T_1^2 \rangle \sin(2\beta_0) \sin(\gamma_0), \quad (5)$$

$$F_{\sigma\text{-}\pi}^{0kl}(\psi) = -\langle T_1^2 \rangle \sin(\alpha_0 - \theta_B) \sin(\gamma_0) \cos(2\beta_0) + \langle T_1^2 \rangle \cos(\alpha_0 - \theta_B) \cos(\gamma_0) \cos(\beta_0), \quad (6)$$

$$F_{\sigma\text{-}\sigma}^{h0l}(\psi) = \langle T_1^2 \rangle \sin(2\beta_0) \cos(\gamma_0), \quad (7)$$

$$F_{\sigma\text{-}\pi}^{h0l}(\psi) = -\langle T_1^2 \rangle \sin(\alpha_0 - \theta_B) \cos(\gamma_0) \cos(2\beta_0) - \langle T_1^2 \rangle \cos(\alpha_0 - \theta_B) \sin(\gamma_0) \cos(\beta_0), \quad (8)$$

where θ_B is the Bragg angle, and $\cotg(\alpha_0) = \cotg(\beta) \sin(\psi)$, $\sin(\beta_0) = \cos(\beta) \cos(\psi)$, $\cotg(\gamma_0) = \cotg(\psi) \sin(\beta)$, $\beta^{0kl} = \arctg(-bl/c)$ and $\beta^{h0l} = \arctg(al/ch)$, where a , b , and c are the lattice constants.

The calculated azimuthal angle dependent scattering intensity for the (033) reflection in both polarization channels is shown in Fig. 2. No interference with the charge term in σ - σ is assumed. The maximum intensities for the two channels are similar. Note that additional charge scattering in σ - σ , allowed in $P2_1/n$ symmetry, may lead to a twofold symmetric azimuthal angle dependence, due to the phase change of the structure factor between the lobes. Moreover, in this phase all second rank tensors contribute. Similar calculations have been published in Ref. 26, but no related experimental results were presented.

IV. RESULTS

Figure 3 shows the energy dependence of the (033) reflection of NdNiO₃ for the σ - σ polarization above and below T_{MI} . Its intensity at $T=20$ K is compared with the charge disproportionation model [Eq. (2) and Ref. 35]. The functions $\Delta f'_{\text{Ni}_I}(E)$ and $\Delta f''_{\text{Ni}_I}(E)$ were used as determined in Ref. 18. For $T > T_{\text{MI}}$, the scattering intensity of the (033) reflection is essentially zero and energy-independent, as expected

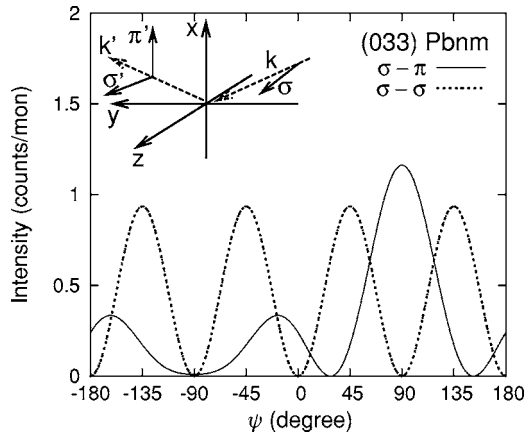


FIG. 2. Calculated azimuthal-angle ψ dependence of the (033) reflection from the anisotropy of the scattering tensor (ATS) contribution of Ni ions in NdNiO_3 with $Pbnm$ symmetry. The σ - σ (dashed line) and σ - π (continuous line) polarization channels have comparable maximum intensity. The inset shows the scattering configuration.

for the high temperature phase with $Pbnm$ symmetry.

Figure 4 displays the energy dependence of the (033) reflection for σ - π for various azimuthal angles. The scattering intensity varies over one order of magnitude between $\psi = -90^\circ$ and $\psi = +90^\circ$. Such a strong modulation is generally attributed to ATS.^{12,13,28} For $F_{\sigma-\pi}^{033}(\psi)$, three prominent features are expected for a full rotation in ψ about the Bragg scattering vector (Fig. 2). For $T=20$ K, as well as for $T=210$ K, three distinct peaks are indeed observed (Fig. 5) at the predicted ψ angles [Eq. (6)]. Qualitative agreement is found between the observed intensity and the calculation for the high temperature phase.

Figure 6 shows the azimuthal angle dependence of the (033) reflection for σ - σ at $T=20$ K. The scattering intensity for σ - σ is essentially independent of the azimuthal angle. This indicates that the scattering due to the charge disproportionation dominates at the (033) reflection, since ATS is ex-

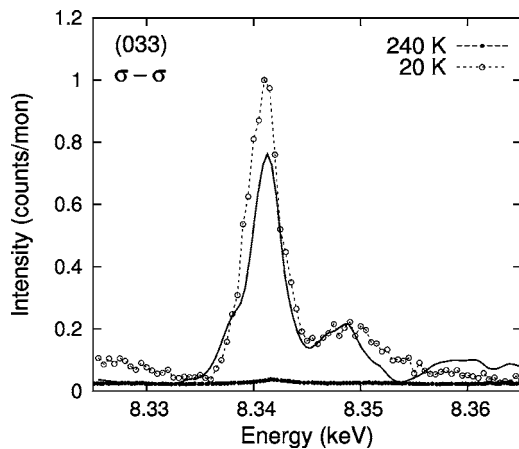


FIG. 3. Normalized intensity of the (033) reflection at $T=20$ K (open circles) and $T=240$ K (filled circles) for the σ - σ polarization ($\psi=10^\circ$). The solid line is a fit to the scattering intensity assuming charge disproportionation.

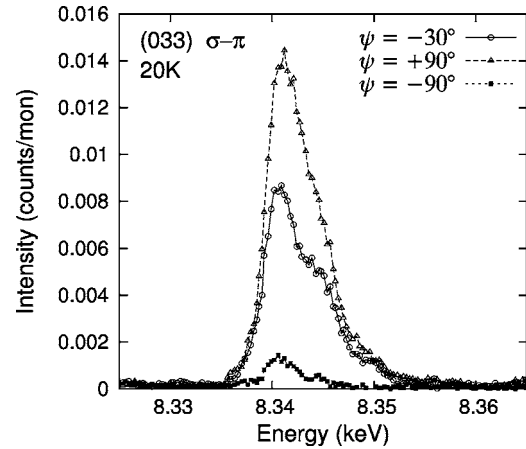


FIG. 4. Normalized intensity of the (033) reflection at $T=20$ K for the σ - π polarization, for three different azimuthal angles.

pected to show a fourfold periodicity [see Eq. (5) and Fig. 2]; we will discuss this in detail in the next section. Figure 7 shows the azimuthal angular dependence of the (105) reflection for σ - π and the prediction of Eq. (8). Again, the σ - π scattered intensity has a strong azimuthal angle dependence which can be attributed to ATS.

The calculated ATS intensities for both σ - π and σ - σ are related to the experimental intensity by a scaling factor proportional to $\langle T_1^2 \rangle$. For the σ - σ channel, the Thomson and ATS structure factors interfere. The absolute intensity contribution of the ATS contribution to this channel can be much larger than the intensity observed for σ - π . Moreover, this may lead to a twofold symmetric behavior in the azimuthal angle dependence. The maximum intensity for the σ - π channel gives an estimate of the maximum expected ATS intensity in the σ - σ channel (Fig. 5); from Fig. 6, the ATS is expected to be at most 5% of the observed signal. The importance of the role of ATS across the metal-insulator transition can be judged from the azimuthal dependence of the (033) reflection for σ - π at $T=20$ and $T=210$ K in Fig. 5. [For (105) see Ref. 36.] The periodicity of the curves remains the same. The

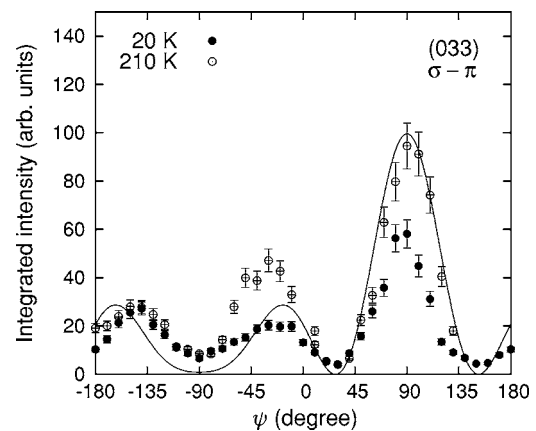


FIG. 5. Azimuthal-angle ψ dependence of the (033) reflection at $T=20$ K (filled circles) and $T=210$ K (open circles) for the σ - π polarization. The solid line is the calculated intensity from the ATS contribution of Ni ions in NdNiO_3 with $Pbnm$ symmetry.

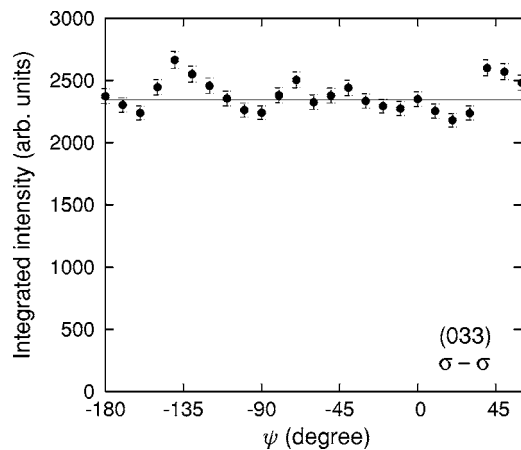


FIG. 6. Azimuthal-angle ψ dependence of the (033) reflection at $T=20$ K for σ - σ polarization. The solid line is a guide to the eye.

general features of the spectrum remain, and only the scattering intensities change. Therefore, the main contribution in this channel originates from the same $\langle T_1^2 \rangle$ tensor. Moreover, the ATS contribution dominates the σ - π channel for $T < T_{MI}$ and $T > T_{MI}$.

V. DISCUSSION

The interpretation of resonant x-ray scattering data can be controversial. The occurrence of reflections of type $(0kl)$ below T_{MI} , may have various origins, e.g., a change of the crystal structure, an enhancement or a decrease of the ATS contribution, Jahn-Teller distortions, or the occurrence of CO or OO. These effects are often related, and therefore may be simultaneously present. In fact, it is difficult to imagine a change in the crystal structure which would not imply a change in the electronic structure of the Ni ions and/or the neighboring oxygen octahedra. In order to evaluate the relative contributions of all these effects, a careful study with polarization analysis and azimuthal scans is essential.

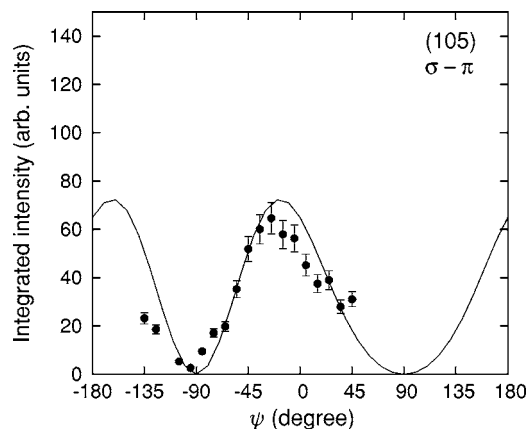


FIG. 7. Azimuthal-angle ψ dependence of the (105) reflection at $T=200$ K for the σ - π polarization. The solid line is the calculated intensity from the anisotropy of the scattering tensor (ATS) contribution of Ni ions in NdNiO_3 with $Pbnm$ symmetry.

TABLE I. Δ_d for selected perovskites above and below the MI phase transition.

Compound	T (K)	$10^4 \times \Delta_d$
NdNiO_3^a	300	0.03 ± 0.01
NdNiO_3^a	170	0.09 ± 0.02
$\text{La}_{1/2}\text{Sr}_{3/2}\text{MnO}_4^b$	300	$1.24 \pm \text{NG}$
$\text{La}_{1/2}\text{Sr}_{3/2}\text{MnO}_4^b$	2	$1.91 \pm \text{NG}$
$\text{Pr}_{0.6}\text{Ca}_{0.4}\text{MnO}_3^c$	280	0.12 ± 0.01
$\text{Pr}_{0.6}\text{Ca}_{0.4}\text{MnO}_3^c$	195	6.748 ± 0.3

^aReference 21.

^bReference 37.

^cReference 38.

First it is important to estimate the distortions of the oxygen octahedra around the resonant Ni ion. The parameter Δ_d is introduced,

$$\Delta_d = \frac{1}{N} \sum_{i=1}^N \left(\frac{R_i - \langle R \rangle}{\langle R \rangle} \right)^2, \quad (9)$$

where N is the number of the oxygen ions bound to the Ni ion, R_i are the Ni-O distances and $\langle R \rangle$ is the average Ni-O bond distance. Table I compares Δ_d for NdNiO_3 with those of other perovskites for which clear evidence for OO exists. For NdNiO_3 , Δ_d is smaller than for the other perovskites. At the phase transition, no appreciable distortion of the octahedra is found. First principle calculations of the OO in manganites indicate that in these compounds, the resonant signal is dominated by the Jahn-Teller distortion.²⁷ A similar situation is expected for NdNiO_3 , and because Δ_d is very small, only a very weak change in the dependence of the ATS at T_{MI} is expected.

Further information can be obtained by comparing the values of Δ_d for the two different phases of each compound. For NdNiO_3 , the change in Δ_d across the transition is at least an order of magnitude smaller than that found in the other materials and is close to the experimental uncertainty. Therefore, NdNiO_3 is an ideal candidate to study OO and CO by means of resonant x-ray scattering, since the contribution of the distortion of the oxygen octahedra to the resonant signal is accordingly small or even negligible. The experimental data presented here shows that this is indeed the case.

Second, the contribution to the scattering factor of non-resonant ions (Nd,O) become nonzero below $T < T_{MI}$, as they move slightly away from the position occupied at $T > T_{MI}$. The reflection then becomes “allowed,” and a Bragg peak will appear. The reflection will not show an energy dependence at the Ni K -edge, and it will be present in the σ - σ channel only. Note that this is not true in general, it applies only when the positions of the resonant ions (Ni in our case) remain unchanged during the reduction in symmetry. If, in addition, ATS is present, the total scattering intensity for σ - σ is the result of the interference of these two terms. This simple explanation does not apply to the (033) reflection of NdNiO_3 below T_{MI} . Even in the case of constructive interference between off-resonance scattering and ATS, the result-

ing intensity would account for only 20% of the observed signal. The (033) and (105) reflections are sensitive to possible differences in the scattering factors of the Ni ions in the unit cell [Eq. (2)]. It is then plausible to interpret the resonant signal observed in the σ - σ channel as being dominated by the spherical contribution of the Ni scattering factors. Therefore, the signal is well described by charge disproportionation of the two Ni sites. The asphericity of the Ni 4*p* states does contribute, but the signal is weak, can only be observed for σ - π , and is essentially temperature independent. This demonstrates that the contribution of additional ATS terms is rather small for $T < T_{\text{MI}}$. Moreover, this indicates that the additional distortion of the oxygen octahedra which occurs at T_{MI} is small and does not significantly change the contribution of ATS to the resonant scattering.

At last, we discuss the possibility of OO below T_{MI} . OO was predicted with the wave vector $k=(1/2\ 0\ 1/2)$.^{22,39} An intensive search for the (*h*/2 0 *l*/2) type reflections was performed, as in Ref. 26, but no scattering was detected for either σ - σ or σ - π . Consequently diffraction attributable to OO in NdNiO₃ is at least three orders of magnitude weaker than that arising from the $\langle T_1^2 \rangle$ quadrupole of the Ni ions.

The Ni $\bar{1}$ site symmetry in *Pbnm* suggest that already in the metallic state the e_g states may be split. The signal in the σ - π channel corresponds to the $\langle T_1^2 \rangle$ quadrupole and gives clear evidence of the asphericity in the 4*p* states induced by the tilt of the oxygen octahedra. This asphericity must cause a similar asphericity of the 3*d* states due to the intra-atomic Coulomb interaction and gives indication that no orbital degeneracy exist above T_{MI} . Therefore no orbital ordering can occur at T_{MI} . In other words, the orbitals are already ordered commensurate to the lattice in the metallic state with *Pbnm* symmetry. The unusual magnetic wave vector is possibly due to an antiferromagnetic next-nearest exchange interaction caused by the charge disproportionation. Alternatively, six equivalent magnetic nearest neighbor exchange interactions can cause a noncollinear magnetic structure as proposed for HoNiO₃.⁴⁰ These results can now be compared with the theoretical prediction of Mizokawa *et al.*²⁰ They have proposed a ground state with charge order on oxygen for the light *R* ions Pr and Nd, and charge ordering on Ni for the heavy *R* ions. The Ni *K*-edge probes directly the Ni 4*p* states. These states are strongly influenced by the oxygen 2*p* overlap as well as by the Ni 3*d* states. Consequently, our results indicate that charge order can occur in the oxygen 2*p* or Ni 3*d* states. However, the proposed theoretical model with charge order-

ing on oxygen is not in accord with a spherical difference of the Ni 4*p* states. It is based on the presence of three oxygen ions with lower and three with higher charge states in the octahedra. Such an order, common to every Ni site, does not give any spherical contribution (i.e., a charge signal in the σ - σ channel) to the Ni 4*p* states as the oxygen contributions cancel each other. However, the model proposed for heavy *R* ions, with CO on Ni, might be applicable also to Nd. Also the model where the charge is located equally in all six Ni-O bonds cannot be excluded as this lead to a spherical coordination of the 4*p* states. We believe that the energy dependence of the measured reflections might differentiate between these two effects. Such a distinction can only be based on detailed electronic calculations, which are beyond the scope of this study. Moreover, these type of calculations require accurate knowledge of the monoclinic distortion, in particular the exact atomic positions of the oxygen ions, which is not the case to date for NdNiO₃.

VI. CONCLUSION

A resonant x-ray scattering study is presented at the Ni *K*-edge that gives clear evidence for charge disproportionation in NdNiO₃. The absence of a significant azimuthal angle dependence of the unrotated signal of the (033) reflection gives clear evidence of the charge origin of the reflection in contrast to the manganites. Therefore, the enhancement is well described by the previously proposed amount of charge disproportionation. The resonant signal in the metallic state in the rotated light channel and its azimuthal angle dependence indicate that the Ni 4*p* shell is aspheric. Consequently, there is no residual orbital degeneracy in the e_g state in the metallic phase. In other words, the orbitals are already ordered, reflected by the tilts of the oxygen octahedra. The small change of this signal at T_{MI} excludes a reorientation of the orbitals to an ordering with a (1/2 0 1/2) wave vector in the insulating state, but is consistent with a small change in the tilting angle of the octahedra. The absence of any reflection of (*h*/2 0 *l*/2) type further confirms this interpretation. The metal-insulator transition in NdNiO₃ is therefore well described by charge disproportionation.

ACKNOWLEDGMENT

This work was supported by the Swiss National Science Foundation.

*Electronic address: valerio.scagnoli@psi.ch

¹J. V. Santen and G. Jonker, *Physica* (Amsterdam) **16**, 599 (1950).

²Y. Moritomo, T. Akimoto, M. Takeo, A. Machida, E. Nishibori, M. Takata, M. Sakata, K. Ohoyama, and A. Nakamura, *Phys. Rev. B* **61**, R13325 (2000).

³A. Maignan, C. Martin, D. Pelloquin, N. Nguyen, and B. Raveau, *J. Solid State Chem.* **142**, 247 (1999).

⁴D. Akahoshi and Y. Ueda, *J. Phys. Soc. Jpn.* **68**, 736 (1999).

⁵P. Lacorre, J. B. Torrance, J. Pannetier, A. I. Nazzal, P. W. Wang, and T. C. Huang, *J. Solid State Chem.* **91**, 225 (1991).

⁶J. B. Torrance, P. Lacorre, A. I. Nazzal, E. J. Ansaldo, and C. Niedermayer, *Phys. Rev. B* **45**, R8209 (1992).

⁷E. Verwey and P. Haaymann *Physica* (Amsterdam) **8**, 979 (1941).

⁸E. Verwey, P. Haaymann, and F. Romeijn, *J. Chem. Phys.* **15**, 181 (1947).

⁹G. Subias, J. Garcia, M. G. Proietti, J. Blasco, H. Renevier, J. L.

- Hodeau, and M. C. Sanchez, Phys. Rev. B **70**, 155105 (2004).
- ¹⁰G. Subias, J. Garcia, J. Blasco, M. GraziaProietti, H. Renevier, and M. ConcepcionSanchez, Phys. Rev. Lett. **93**, 156408 (2004).
- ¹¹J. Garcia, M. C. Sanchez, G. Subias, and J. Blasco, J. Phys.: Condens. Matter **13**, 3229 (2001).
- ¹²S. Grenier *et al.*, Phys. Rev. B **69**, 134419 (2004).
- ¹³J. Herrero-Martin, J. Garcia, G. Subias, J. Blasco, and M. ConcepcionSanchez, Phys. Rev. B **70**, 024408 (2004).
- ¹⁴Y. Murakami, H. Kawada, H. Kawata, M. Tanaka, T. Arima, Y. Moritomo, and Y. Tokura, Phys. Rev. Lett. **80**, 1932 (1998).
- ¹⁵Y. Murakami *et al.*, Phys. Rev. Lett. **81**, 582 (1998).
- ¹⁶J. B. Goodenough, Phys. Rev. **100**, 564 (1955).
- ¹⁷J. A. Alonso, J. L. Garcia-Munoz, M. T. Fernandez-Diaz, M. A. G. Aranda, M. J. Martinez-Lope, and M. T. Casais, Phys. Rev. Lett. **82**, 3871 (1999).
- ¹⁸U. Staub, G. I. Meijer, F. Fauth, R. Allenspach, J. G. Bednorz, J. Karpinski, S. M. Kazakov, L. Paolasini, and F. d'Acapito, Phys. Rev. Lett. **88**, 126402 (2002).
- ¹⁹M. Imada, A. Fujimori, and Y. Tokura, Rev. Mod. Phys. **70**, 1039 (1998).
- ²⁰T. Mizokawa, D. I. Khomskii, and G. A. Sawatzky, Phys. Rev. B **61**, 11263 (2000).
- ²¹J. L. Garcia-Munoz, J. Rodriguez-Carvajal, P. Lacorre, and J. B. Torrance, Phys. Rev. B **46**, 4414 (1992).
- ²²J. Rodriguez-Carvajal, S. Rosenkranz, M. Medarde, P. Lacorre, M. T. Fernandez-Diaz, F. Fauth, and V. Trounov, Phys. Rev. B **57**, 456 (1998).
- ²³M. Medarde, J. Phys.: Condens. Matter **9**, 1679 (1997).
- ²⁴J. Rodriguez-Carvajal, M. Hennion, F. Moussa, A. H. Moudden, L. Pinsard, and A. Revcolevschi, Phys. Rev. B **57**, R3189 (1998).
- ²⁵In *Pbnm* symmetry, Ni ions have multiplicity 4; positions are $R_1=(1/2\ 0\ 0)$, $R_2=(0\ 1/2\ 0)$, $R_3=(1/2\ 0\ 1/2)$, $R_4=(0\ 1/2\ 1/2)$; in *P2₁/n* symmetry, Ni_I sits at sites 1 and 4 and Ni_{II} is at 2 and 3.
- ²⁶J. E. Lorenzo, J. L. Hodeau, L. Paolasini, S. Lefloch, J. A. Alonso, and G. Demazeau, Phys. Rev. B **71**, 045128 (2005).
- ²⁷M. Benfatto, Y. Joly, and C. R. Natoli, Phys. Rev. Lett. **83**, 636 (1999).
- ²⁸H. Nakao, Y. Wakabayashi, T. Kiyama, Y. Murakami, M. v. Zimmermann, J. P. Hill, D. Gibbs, S. Ishihara, Y. Taguchi, and Y. Tokura, Phys. Rev. B **66**, 184419 (2002).
- ²⁹M. Kubota, H. Nakao, Y. Murakami, Y. Taguchi, M. Iwama, and Y. Tokura, Phys. Rev. B **70**, 245125 (2004).
- ³⁰S. B. Wilkins, P. D. Spencer, P. D. Hatton, S. P. Collins, M. D. Roper, D. Prabhakaran, and A. T. Boothroyd, Phys. Rev. Lett. **91**, 167205 (2003).
- ³¹D. J. Huang *et al.*, Phys. Rev. Lett. **92**, 087202 (2004).
- ³²S. S. Dhesi *et al.*, Phys. Rev. Lett. **92**, 056403 (2004).
- ³³D. Templeton and L. Templeton, Acta Crystallogr., Sect. A: Cryst. Phys., Diffir., Theor. Gen. Crystallogr. **36**, 237 (1980).
- ³⁴J.-S. Zhou and J. B. Goodenough, Phys. Rev. B **69**, 153105 (2004).
- ³⁵V. Scagnoli, U. Staub, M. Janousch, G. I. Meijer, L. Paolasini, F. D'Acapito, J. G. Bednorz, and R. Allenspach, J. Magn. Magn. Mater. **272**, 420 (2004).
- ³⁶U. Staub, V. Scagnoli, M. Janousch, G. I. Meijer, L. Paolasini, F. D'Acapito, J. G. Bednorz, R. Allenspach, and S. W. Lovesey, Physica B **345**, 23 (2004).
- ³⁷J. Bouloux, J. Soubeyroux, A. Daoudi, and G. L. Flem, Mater. Res. Bull. **16**, 855 (1981).
- ³⁸A. Daoud-Aladine, J. Rodriguez-Carvajal, L. Pinsard-Gaudart, M. T. Fernandez-Diaz, and A. Revcolevschi, Phys. Rev. Lett. **89**, 097205 (2002).
- ³⁹J. L. Garcia-Munoz, J. Rodriguez-Carvajal, and P. Lacorre, Phys. Rev. B **50**, 978 (1994).
- ⁴⁰M. T. Fernandez-Diaz, J. A. Alonso, M. J. Martinez-Lope, M. T. Casais, and J. L. Garcia-Munoz, Phys. Rev. B **64**, 144417 (2001).